Gas stripping by radiation drag from an interstellar cloud

Jun'ichi Sato,[1]★ Masayuki Umemura,[1]★ Keisuke Sawada[2]★ and Shingo Matsuyama[3]★

[1]*Centre for Computational Sciences, University of Tsukuba, Tsukuba 305-8577, Japan*
[2]*Department of Aeronautics and Space Engineering, Tohoku University, Sendai 980-8579, Japan*
[3]*Institute of Space Technology and Aeronautics, AXA, Chofu 182-8522, Japan*

ABSTRACT

We perform two-dimensional hydrodynamic simulation of gas stripping by radiation drag from interstellar clouds moving in uniform radiation fields. To include relativistic radiation drag properly, the radiation hydrodynamic equation is solved taking into account the dilution of radiation fields by the optical depth of the cloud. As a result, it is found that the optically thin surface layers are effectively stripped by radiation drag from an optically thick gas cloud, and, simultaneously, the stripped gas loses momentum. The momentum loss time-scale is found to be on the order of 10^8 yr under the intensive radiation fields expected in the early phase of galaxy evolution. The present results show that the radiation drag is an effective mechanism for extracting angular momentum from the interstellar medium and allows it to accrete on to the galactic centre. Mass accretion driven by radiation drag may lead to the formation of a central supermassive black hole.

Key words: black hole physics – hydrodynamics – methods: numerical – galaxies: bulges – galaxies: nuclei – galaxies: starburst.

1 INTRODUCTION

When matter moves in radiation fields, it absorbs radiation anisotropically in the comoving frame and then re-emits the radiation isotropically, so that the gas is subject to a drag force in proportion to vE, where v is the peculiar velocity and E is the radiation energy density (Mihalas & Mihalas 1984). This effect is known as radiation drag. A famous example of radiation drag is the Poynting–Robertson effect on dust grains in the Solar System (Poynting 1903; Robertson 1937), where, owing to angular momentum loss caused by the radiation drag, the grains spiral into the Sun.

The importance of radiation drag has been considered in the case of various other issues in astrophysics. In the epochs shortly after recombination, the cosmic background radiation could exert a strong drag force through electron scattering, which is called Compton drag. Loeb (1993) considered the possibility that the Compton drag could extract angular momentum from an early formed object and build up a massive black hole. In this context, Umemura, Loeb & Turner (1993) performed numerical simulations, using a three-dimensional hydrodynamics–dark matter code, and found that the angular momentum extraction actually takes place efficiently at redshifts of $z \gtrsim 300$, leading to the formation of massive black holes.

Radiation drag-induced mass accretion is also considered in a rotating gas disc immersed in external radiation fields. Cosmological accretion discs embedded in background radiation have been ex-

tensively studied by Fukue & Umemura (1994), Tsuribe, Fukue & Umemura (1994), Umemura & Fukue (1994), Tsuribe & Umemura (1997) and Mineshige, Tsuribe & Umemura (1998). In relation to quasi-periodic phenomena in X-ray stars, Fortner, Lamb & Miller (1989), Lamb (1989, 1991) and Miller & Lamb (1993) examined the role of radiation (Compton) drag exerted by the radiation fields of a central neutron star on the disc gas in the binary regime. Meyer & Meyer-Hofmeister (1994) proposed siphon processes in cataclysmic variables, where the evaporating gas from the disc surface infalls toward a central white dwarf because of radiation drag. Fukue & Umemura (1995) investigated a steady accretion driven by the radiation of a central luminous object. Also, in active galactic nuclei (AGNs), the radiation drag may play an important role in some situations. Umemura, Fukue & Mineshige (1997) proposed starburst-induced fuelling of an AGN ('radiative avalanche'), to relate the circumnuclear starburst to an AGN event. This model has been extended to more realistic versions (Fukue, Umemura & Mineshige 1997; Umemura, Fukue & Mineshige 1998; Ohsuga et al. 1999). Commonly, it was found that the surface layer of rotating gas irradiated by intensive starlight can lose angular momentum by radiation drag, which results in an avalanche in the layer as an inevitable consequence.

The model of mass accretion induced by uniform background radiation is revitalized in galactic bulges, because bulge stars produce nearly uniform radiation fields. This can provide a possible way to cause the formation of a supermassive black hole (SMBH) in a bulge. Recent observations have suggested that the mass of an SMBH tightly correlates with the mass of the host bulge or the velocity dispersion of bulge stars (Kormendy & Richstone

★E-mail: junichi@rccp.tsukuba.ac.jp (JS); umemura@rccp.tsukuba.ac.jp (MU); sawada@cfd.mech.tohoku.ac.jp (KS); smatsu@chofu.jaxa.jp (SM)

1995; Miyoshi et al. 1995; Laor 1998; Magorrian 1998; Richstone et al. 1998; Ho 1999; Wandel 1999; Ferrarese & Merritt 2000; Gebhardt et al. 2000a,b; Kormendy & Ho 2000; Merrifield, Forbes & Terlevich 2000; Nelson 2000; Salucci et al. 2000; Ferrarese et al. 2001; McLure & Dunlop 2001; Merritt & Ferrarese 2001a,b; Sarzi et al. 2001; McLure & Dunlop 2002; Wandel 2002). All of these correlations imply that the formation of an SMBH is likely to be physically linked to the formation of a galactic bulge that harbours an SMBH. Umemura (2001) considered the accretion of dusty gas driven via the radiation drag by bulge stars and constructed a quasar formation model. Kawakatu & Umemura (2002) quantitatively clarified by radiative transfer calculations that the inhomogeneity of a dusty interstellar medium controls the efficiency of radiation drag, and found that, if surface gas layers are stripped effectively by the radiation drag from optically thick dusty gas clouds and lose angular momentum, a sufficient amount of gas can accrete to form an SMBH in realistic situations. The model of radiation drag-induced formation of SMBHs predicts the SMBH-to-bulge mass relation to be $0.3–0.5\varepsilon$, where ε is the fraction of mc^2 liberated by hydrogen burning in stars. However, the processes of gas stripping by the radiation drag from an optically thick cloud have not been elucidated in detail. The study requires a sophisticated numerical simulation with relativistic radiation hydrodynamics. In this paper, we perform a radiation hydrodynamic simulation with generalized coordinates for a gas cloud moving in radiation fields. Through this simulation, we attempt to demonstrate the stripping efficiency and the time-scale of angular momentum loss of the gas.

The paper is organized as follows. In Section 2, we present the model used in this work. In Section 3, we describe the numerical treatment. In Section 4, we show the numerical results on the flow patterns and then estimate the time-scale for momentum loss of the gas. Section 5 is devoted to conclusions.

2 MODEL

We suppose a simple situation in which a spherical cold gas cloud moves in uniform radiation fields with a constant velocity. The gas cloud is assumed to have a uniform density distribution and to be in pressure balance with hot rarefied ambient gas. If there is a relatively large velocity difference between the gas cloud and the ambient matter, the cloud surface layers are expected to be stripped by the ram pressure. The ram pressure stripping itself does not extract angular momentum from the total system including the cloud and ambient matter. But, if the system is embedded in radiation fields, the optically thin parts of the stripped gas can be subject to the radiation drag and lose angular momentum. This might provide a simple way to extract angular momentum from the interstellar medium. From a realistic point of view, however, the gas motion does not seem so simple. Recent high-resolution simulations on multiple supernova (SN) explosions in a star-forming galaxy (Mori, Umemura & Ferrara 2004) have revealed that dense shells driven by SN hot bubbles undergo thermal instability and the resultant cold clouds move together with ambient hot gas. Here, we consider two cases; one is a comoving case in which the stripping takes place solely by the radiation drag, and the other is a shear-flow case in which the radiation drag is partially coupled with the ram pressure stripping. The comoving case can correspond to the early phase of the fragmentation of a hot bubble-induced dense shell. But, shortly after the fragmentation, velocity difference is expected to arise between a dense fragment and hot ambient gas. Hence, the shear-flow case seems more plausible from a realistic viewpoint. (A radiation drag-dominant case without noticeable ram pressure

effects may occur when gas clouds are assembled in early formed objects exposed to intensive cosmic background radiation at quite high-redshift epochs – see, for example, Loeb 1993.)

The cloud temperature, mass and radius are respectively assumed to be $T_c = 10^2$ K, $M_c = 3.0 \times 10^5$ M$_\odot$ and $R_c = 10$ pc, while the temperature of hot ambient matter is $T_h = 10^7$ K. We postulate the peculiar velocity v_p of the cloud to be of the order of the virial velocity for a spheroidal galaxy with $M_{tot} = 10^{11}$ M$_\odot$ and $R_g = 1$ kpc:

$$v_{vir} = 6.67 \times 10^2 \text{ km s}^{-1} \left(\frac{M_{tot}}{10^{11} M_\odot} \right)^{1/2} \left(\frac{R_g}{1 \text{kpc}} \right)^{-1/2}. \quad (1)$$

As for the radiation fields, the radiation energy density is estimated by the assumed total luminosity L_* and galaxy size to be

$$E = \frac{L_*}{4\pi R_g^2 c} = 3.45 \times 10^{-2} \text{ erg cm}^{-3}$$
$$\times \left(\frac{L_*}{3 \times 10^{12} L_\odot} \right) \left(\frac{R_g}{1 \text{ kpc}} \right)^{-2}. \quad (2)$$

In this paper we assume the total luminosity to be $L_* = 3 \times 10^{12}$ L$_\odot$.

3 METHOD OF CALCULATION

We use the two-dimensional generalized curvilinear coordinates shown in Fig. 1. The number of grid points is 101×101. Such coordinates allow us to take accurate boundary conditions for a spherical gas cloud and also to treat appropriately the flow of stripped gas on the right-hand side. The scale of the computational domain is about 50 pc. The gas cloud moves at a velocity v_p along the x-axis in the radiation fields. Here, to prevent the cloud from going out of the boundary with v_p, we make the Galilean transformation by v_p so that the cloud should stay at the origin if neither drag force nor ram pressure is exerted. In these coordinates, the surface of the cold gas is represented by a dash–dotted line in Fig. 1. The other regions are filled with hot gas.

The two-dimensional Euler equations including the relativistic radiation drag term can be written in the conservation form as

$$\frac{\partial \tilde{Q}}{\partial t} + \frac{\partial \tilde{F}}{\partial x} + \frac{\partial \tilde{G}}{\partial y} + \tilde{H} = 0, \quad (3)$$

where $\tilde{Q}$, $\tilde{F}$, $\tilde{G}$ and $\tilde{H}$ are respectively the following vectors,

$$\tilde{Q} = \begin{pmatrix} \rho \\ \rho u \\ \rho v \\ e \end{pmatrix}, \quad \tilde{F} = \begin{pmatrix} \rho u \\ \rho u^2 + p \\ \rho u v \\ (e + p)u \end{pmatrix},$$

$$\tilde{G} = \begin{pmatrix} \rho v \\ \rho u v \\ \rho v^2 + p \\ (e + p)v \end{pmatrix},$$

$$\tilde{H} = \begin{pmatrix} 0 \\ \rho \chi E(u - v_p)/c \\ \rho \chi E v/c \\ 0 \end{pmatrix}, \quad (4)$$

where ρ is the density of the gas, u and v are respectively the x- and y-components of velocity, c is the speed of light, and χ is the mass extinction coefficient due to dust opacity. In this work, we set $\chi = 100$ cm^2 g^{-1} by assuming the Solar abundance and 0.1 μm dust grains (see, for example, Umemura et al. 1998). The pressure
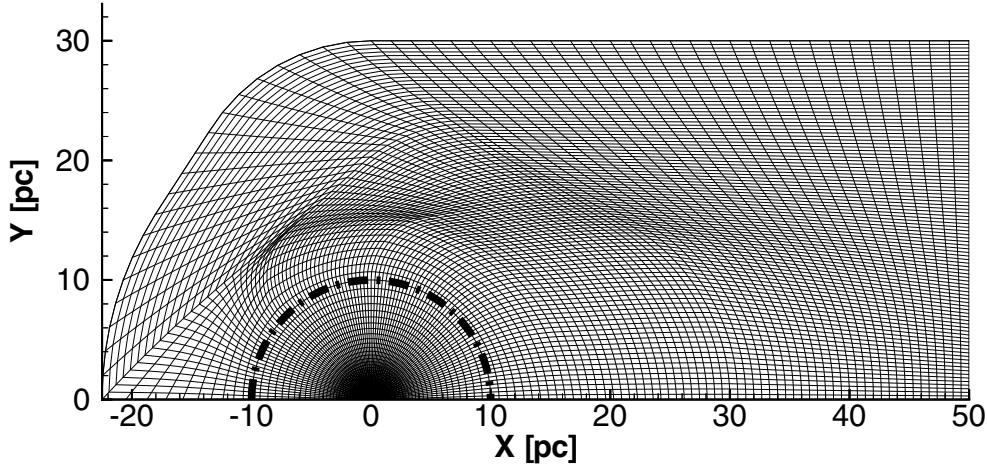
Figure 1. The two-dimensional generalized curvilinear coordinate used here. The number of grid points is 101×101. The surface of the cold gas is represented by a dash–dotted line.

p and the total energy per unit volume e are related by the equation of state,

$$p = (\gamma - 1) \left[e - \frac{\rho}{2}(u^2 + v^2) \right], \tag{5}$$

where γ is the ratio of specific heats of the gas, which is chosen as $\gamma = 5/3$. The radiation drag effect is taken into account by adding the term $\tilde{H}$.

To discretize the governing equation, equation (3), the finite volume approach is used, where the AUSM-DV scheme is employed to obtain the numerical convective flux (Wada & Liou 1994). The time integration of a set of equations is performed implicitly by a matrix-free LU-SGS method (Nakahashi et al. 1999).
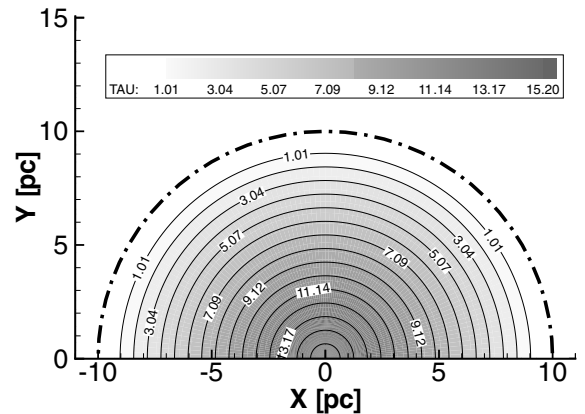
The optical depth at each point is evaluated by integrating the opacity along a line drawn from the outer boundary to the coordinate origin. The distribution of the optical depth in the cloud at the initial time is shown in Fig. 2. The optical depth at the centre of cloud reaches above 15 and the thickness of the optically thin surface layer is $\sim$10 per cent of the cloud radius. We involve the radiation drag term if the optical depth is lower than unity, because no drag force works in an optically thick medium (Tsuribe & Umemura 1997).

In order to demonstrate the validity of the present method for the optical depth estimation, we show the optical depth distributions on several snapshots of the dynamical evolution in Fig. 3. The dot–dashed semicircle shows the initial position of the cloud. The light grey or charcoal grey regions show the domain where the optical depth is from 0.1 to 1 or above 1, respectively. The optically thin regions are properly detected by tracing the dynamical evolution. The gas in charcoal grey regions is impervious to the radiation drag. However, there is a limitation to the application of this method. If the whole region of the cold gas deviates from the coordinate origin, the estimate of optical depth would not be correct. Therefore, at this time, the estimate of the radiation drag is not always accurate. In Section 4 we will return to this point.

4 RESULTS

4.1 Comoving case

Stripping purely by radiation drag is demonstrated in a comoving case, where no relative velocity is present between the gas cloud
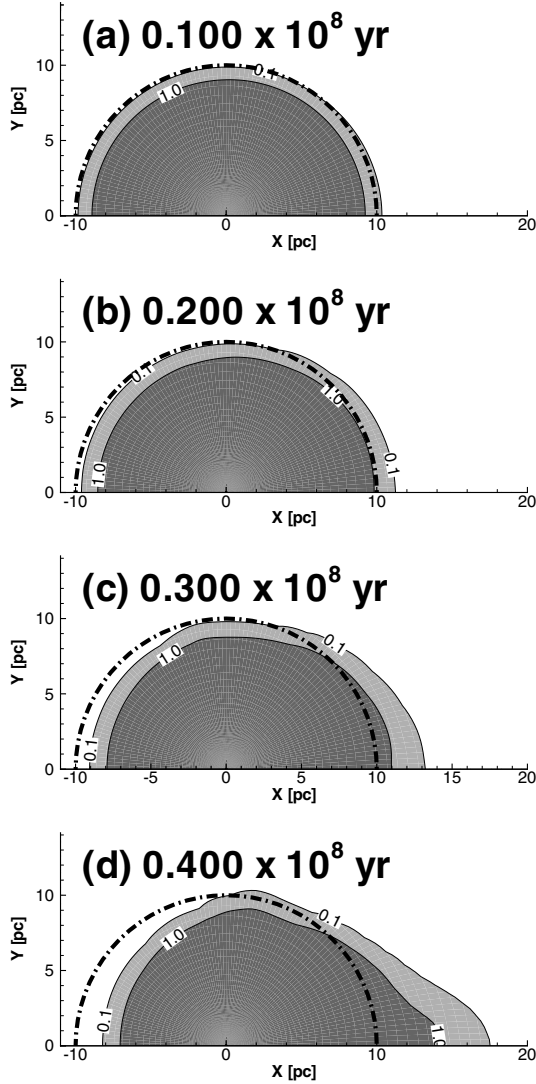

Figure 2. The distribution of the optical depth in the vicinity of the cold gas at initial time. The optical depth at each point is evaluated by integrating the opacity along with a line drawn from the outer boundary to the coordinate origin. The surface of the cold gas is represented by a dash–dotted line.

and the ambient matter. The time variation of density distributions is depicted by four snapshots in Fig. 4, and that of the velocity fields is shown only for optically thin cold gas in Fig. 5, in which the density contours are also displayed. We can see in Fig. 4 that the surface layers of the gas cloud have been stripped by radiation drag and have drifted to the right-hand side. Since we are observing the phenomenon in coordinates moving to the left at velocity v_p, the gas that has drifted to the right has actually been left behind by the radiation drag. It is noted that this stripping is obviously different from the ram pressure stripping in that it occurs also behind the cloud in the downstream. The left-hand side of the optically thin surface layer pushes the whole region to the right by radiation drag.

The velocity fields in Fig. 5 show that the optically thin surface layers move round the surface of the cloud. A part of the gas reaching the x-axis is accelerated toward the right direction along the x-axis. This means that the stripped gas is slowed down by the radiation drag.

In the later phase ($t > 10^8$ yr), the stripped gas is trailed by the radiation drag, because the cold gas is confined by the ambient hot gas. When the stripped gas reaches the x-axis, it splits into left and right under the influence of external pressure. The radiation drag is

(a) 0.100 x 10⁸ yr

(b) 0.200 x 10⁸ yr

(c) 0.300 x 10⁸ yr

(d) 0.400 x 10⁸ yr

Figure 3. The optical depth distributions on several snapshots of the dynamical evolution. The dot–dashed semicircle shows the initial position of the cloud. The light grey or charcoal grey regions show the domain where the optical depth is from 0.1 to 1 or above 1, respectively. The gas in light grey is subject to the radiation drag, while that in charcoal grey regions is impervious to the radiation drag.

not exerted on the gas splitting into the left owing to the large optical depth and therefore left there in the present Galilean-transformed coordinates, while the radiation drag works to decelerate the optically thin gas splitting to the right and eventually produces the gas flows to the right. As mentioned before, when the whole region of the cloud deviates from the origin, the present estimate of the optical depth in the left-hand side of the cloud becomes inaccurate. However, as far as the gas drifting to the right is concerned, the optical depth is still properly estimated. Hence, the trailing flow is thought to be real.

4.2 Shear-flow case

Here, we show the results for a shear-flow case in which the velocity difference between the gas cloud and the ambient matter is assumed to be $0.1v_p$, corresponding to Mach number 0.13. The numerical results are shown in Figs 6 and 7, respectively, for the density distributions and the velocity fields for the optically thin cold gas.

(a) 0.100 x 10⁸ yr

(b) 0.388 x 10⁸ yr

(c) 0.504 x 10⁸ yr

(d) 1.252 x 10⁸ yr
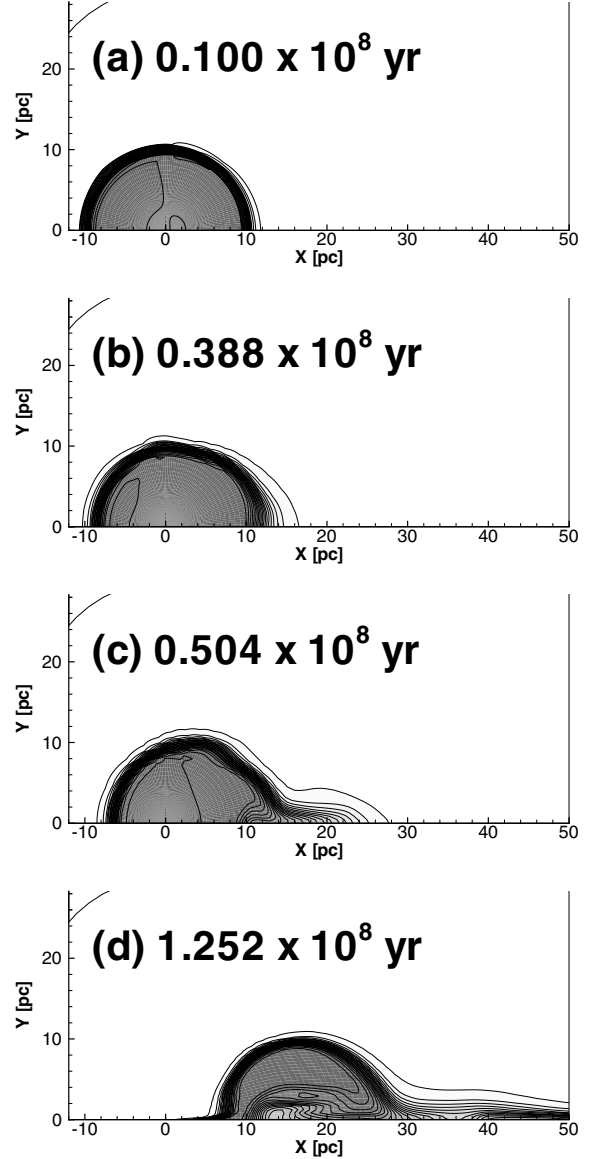
Figure 4. The time variation of density distributions in a comoving case. (a), (b), (c) and (d) show these at times 0.100×10^8, 0.388×10^8, 0.504×10^8 and 1.252×10^8 yr, respectively. The density range is from 3.5×10^{-23} to 5.3×10^{-21} g cm^{-3}. Each density range is divided by 21 lines with equal increments.

The snapshots of the density contours in Fig. 6 show that the deformation of the gas cloud grows with time. In this case, the ram pressure stripping occurs simultaneously with the stripping driven by the radiation drag. However, as shown in Fig. 6(d), the gas drifting to the right eventually flows along with the *x*-axis. This flow pattern is similar to that in the case without ram pressure induced deformation.

The snapshots of the velocity fields show that the rightward velocities of the optically thin surface layers increase with the deformation. Our numerical method allows us to trace the optically thin surface even with such strong deformation of the cold gas. The optically thin gas is subject to the radiation drag and makes a trailing flow, similar to the case without the ram pressure.

4.3 Momentum loss

The radiation drag works on both radial and azimuthal components of gas velocity, in proportion to each component. In a pure rotating
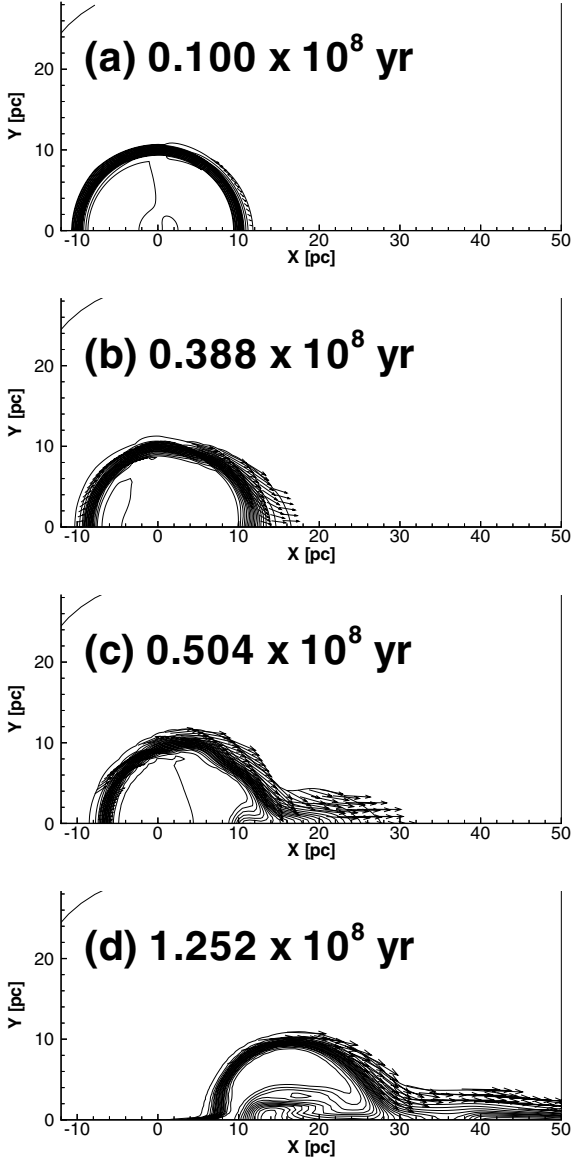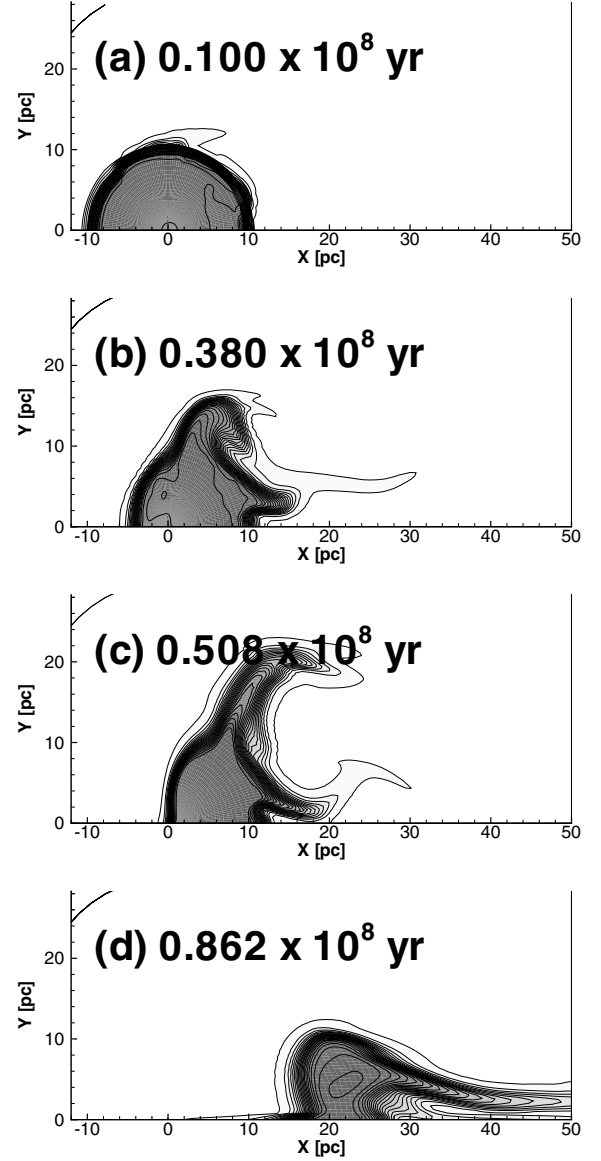
Figure 5. The time variation of vector fields for the optically thin cold gas in a comoving case. (a), (b), (c) and (d) show the flow patterns at the same stages as Fig. 4, respectively. The density contours are also displayed. The density range and the number of contour lines are also the same as in Fig. 4.

Figure 6. The time variation of density distributions in a shear-flow case. (a), (b), (c) and (d) show these at times 0.100×10^8, 0.380×10^8, 0.508×10^8 and 0.862×10^8 yr, respectively. The density range and the number of contour lines are the same as in Fig. 1.

system, the reduction only for azimuthal velocity leads to the angular momentum loss. But, in a chaotic system like a bulge under starbursts, the reduction of random velocities means, on average, the decrease of an azimuthal component of velocity and therefore angular momentum. In other words, the gas even in non-radial motion can fall in to the centre if the momentum of the gas is strongly reduced. Hence, here we consider the momentum loss in the present simulations. The momentum of optically thin cold gas in the x-direction, Q_x, is defined as

$$Q_x \equiv \int_{\tau \leqslant 1} \rho |u - v_p| \, dV. \tag{6}$$

In Fig. 8, the time variation of momentum is shown in units of the initial momentum. The solid line is the evolution in a comoving case, while the broken line is in a shear-flow case. A dotted line shows the level of $1/e$ reduction.
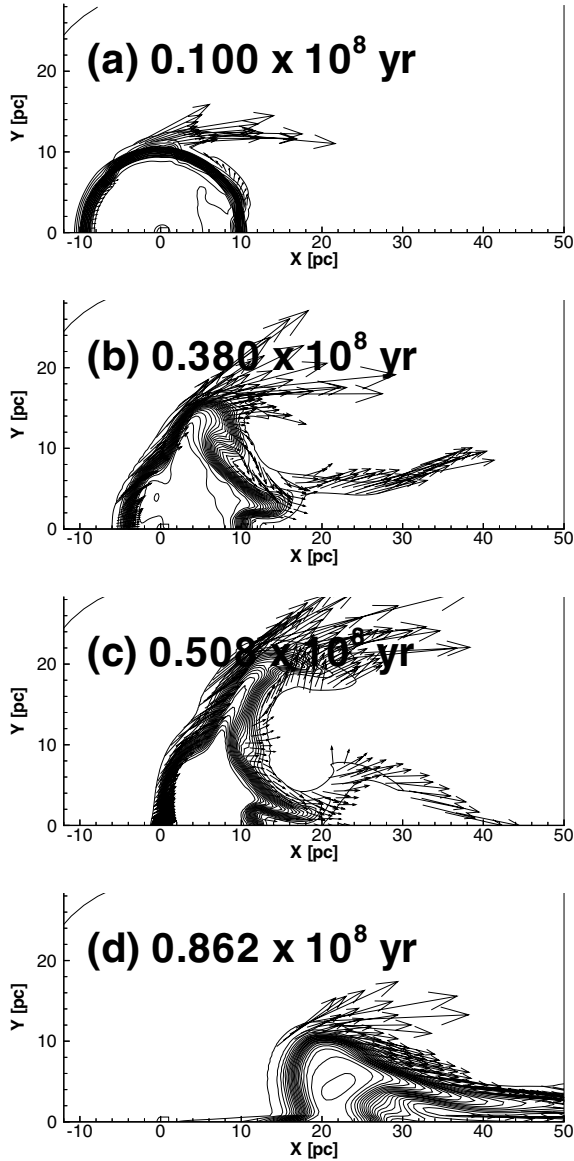
From this result, we can evaluate the momentum loss time-scale, which is defined by the $1/e$ reduction of momentum. The time-scale for a comoving case is $t = 1.04 \times 10^8$ yr, and that for a shear-flow case is $t = 0.8 \times 10^8$ yr. In the shear-flow case, the surface gas of the cloud is also stripped by the ram pressure and is rarefied. As a result, the fraction of optically thin gas increases compared with the pure radiation drag case, so that the momentum is extracted more efficiently than in the comoving case.

The time-scale of angular momentum extraction has been estimated analytically by Umemura et al. (1998) to give

$$t_\gamma \simeq 2.4 \times 10^8 \text{ yr} \left(\frac{L_*}{3 \times 10^{12} \, \text{L}_\odot} \right)^{-1} \left(\frac{R_g}{1 \, \text{kpc}} \right)^2$$

$$\times \left(\frac{f_{dg}}{10^{-1}} \right)^{-2} \left(\frac{a_d}{0.1 \, \mu\text{m}} \right) \left(\frac{\rho_s}{\text{g cm}^{-3}} \right), \tag{7}$$

Figure 7. The time variation of vector fields for the optically thin cold gas in a shear-flow case. (a), (b), (c) and (d) show the flow patterns at the same stages as in Fig. 6, respectively. The density contours are also displayed. The density range and the number of contour lines are the same as in Fig. 4.

where f_{dg}, a_d and ρ_s are the dust-to-gas mass ratio, the grain radius, and the density of solid material within the grain, respectively. It is found that the numerically obtained time-scale is in a good agreement with the analytic estimate, although the numerical one is slightly shorter.

5 CONCLUSIONS AND DISCUSSION

We have performed the radiation–hydrodynamic simulation for a gas cloud moving at a constant velocity in uniform radiation fields, with focusing attention on the radiation drag as well as the coupling effect with ram pressure. The results obtained are summarized as follows.

(i) In a comoving case, the stripping occurs purely through the radiation drag. All the optically thin surface layers are stripped from
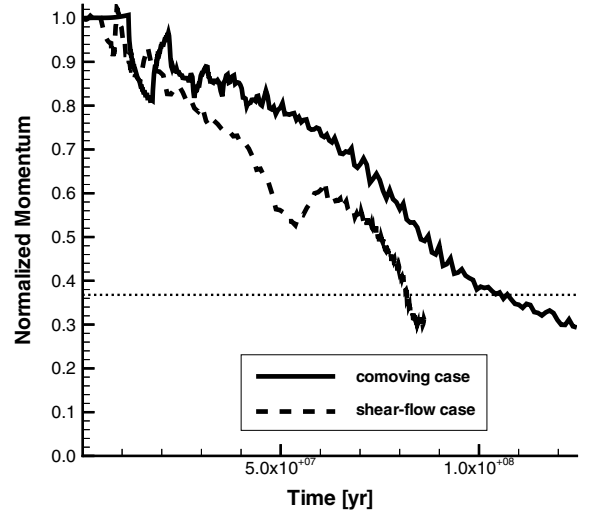
Figure 8. The time variation of momentum in units of the initial momentum. The solid line is the evolution in a comoving case, while the broken line is in a shear-flow case. A dotted line shows the level of $1/e$ reduction.

an optically thick gas cloud, in contrast to the pure ram pressure stripping. Finally, a trailing flow behind the cloud forms.

(ii) In a shear-flow case, the radiation drag-induced stripping occurs simultaneously with the ram pressure stripping. But, the eventual flow pattern for optically thin gas is similar to the pure radiation drag case.

(iii) The momentum loss time-scale for the stripped gas is on the order of 10^8 yr under the intensive radiation fields expected in an early evolutionary phase of a massive bulge. The time-scale is shorter for a shear-flow case with the aid of ram pressure. The present time-scale is basically in good agreement with an analytic estimation of the angular momentum extraction time-scale.

It is demonstrated that the radiation drag by bulge stars is an effective mechanism to extract angular momentum from interstellar clouds in a galactic bulge system. This mechanism allows mass accretion on to the galactic centre, possibly leading to the formation of a supermassive black hole (Umemura 2001; Kawakatu & Umemura 2002; Kawakatu, Umemura & Mori 2003; Kawakatu & Umemura 2004).

In the present work, we have ignored the effect of self-gravity. Self-gravity is likely to be important for a cloud with $M_c = 3.0 \times 10^5 \, M_\odot$, assumed in the present paper. Thus, the assumption of a uniform cloud may not be realistic, and instead the density distribution of a cold gas in gravitational equilibrium should be considered. In this case, the outside of a gas cloud could be rarefied and the domain of the optically thin layers increases. Consequently, the efficiency of the radiation drag might be enhanced. To investigate the details of the stripping and momentum loss in such a case will be significant in future work.

REFERENCES

Ferrarese L., Merritt D., 2000, ApJ, 539, L9
Ferrarese L., Pogge R. W., Peterson B. M., Merritt D., Wandel A., Joseph C. L., 2001, ApJ, 555, L79
Fortner B. A., Lamb F. K., Miller G. S., 1989, Nat, 342, 775
Fukue J., Umemura M., 1994, PASJ, 46, 87
Fukue J., Umemura M., 1995, PASJ, 47, 429
Fukue J., Umemura M., Mineshige S., 1997, PASJ, 49, 673
Gebhardt et al., 2000a, ApJ, 539, L13
Gebhardt et al., 2000b, ApJ, 543, L5
Ho L. C., 1999, in Chakrabarti S. K., ed., Observational Evidence for Black Holes in the Universe. Kluwer, Dordrecht, p. 157
Kawakatu N., Umemura M., 2002, MNRAS, 329, 572
Kawakatu N., Umemura M., 2004, ApJ, 601, 21
Kawakatu N., Umemura M., Mori M., 2003, ApJ, 583, 85
Kormendy J., Richstone D., 1995, ARA&A, 33, 581
Kormendy J., Ho L. C., 2000, Encyclopedia of Astronomy and Astrophysics
Lamb F. K., 1989, in 23rd ESLAB Symposium, p. 215
Lamb F. K., 1991, in Venturam J., Pines D., eds, Neutron Stars: Theory and Observations. Kluwer Academic, Dordrecht, p. 445
Laor A., 1998, ApJ, 505, L83
Loeb A., 1993, ApJ, 403, 542
McLure R. J., Dunlop J. S., 2001, MNRAS, 327, 199
McLure R. J., Dunlop J. S., 2002, MNRAS, 331, 795
Magorrian J. et al., 1998, ApJ, 115, 2285
Merrifield M. R., Forbes D. A., Terlevich A. I., 2000, MNRAS, 313, L29
Merritt D., Ferrarese L., 2001a, MNRAS, 320, L30
Merritt D., Ferrarese L., 2001b, ApJ, 547, 140
Meyer F., Meyer-Hofmeister E., 1994, A&A, 288, 175
Mihalas D., Mihalas B. W., 1984, in Foundations of Radiation Hydrodynamics. Oxford Univ. Press, Oxford, section 7
Miller G. S., Lamb F. K., 1993, ApJL, 414, L43
Mineshige S., Tsuribe T., Umemura M., 1998, PASJ, 50, 233
Miyoshi M., Morton J., Herrnstein J., Greenhill L., Nakai N., Diamond P., Inoue M., 1995, Nat, 373, 127
Mori M., Umemura M., Ferrara A., 2004, PASA, 21, 232
Nakahashi K., Sharov D., Kano S., Kodera M., 1999, Int. J. Numer. Meth. Fluids, 31, 97
Nelson C. H., 2000, ApJ, 544, L91
Ohsuga K., Umemura M., Fukue J., Mineshige S., 1999, PASJ, 51, 345
Poynting J. H., 1903, Phil. Trans R. Soc. London, Ser A, 202, 252
Richstone D. et al., 1998, Nat, 395A, 14
Robertson H. P., 1937, MNRAS, 97, 423
Salucci P., Ratnam C., Monaco P., Danse L., 2000, MNRAS, 317, 488
Sarzi M., Rix H.-W., Shields C., Rudnick G., Ho L. C., McIntosh D. H., Filippenko A. V., Sargent W. L. W., 2001, ApJ, 550, 65
Tsuribe T., Umemura M., 1997, ApJ, 486, 48
Tsuribe T., Fukue J., Umemura M., 1994, PASJ, 46, 597
Umemura M., 2001, ApJ, 560, L29
Umemura M., Fukue J., 1994, PASJ, 46, 567
Umemura M., Loeb A., Turner E. L., 1993, ApJ, 419, 459
Umemura M., Fukue J., Mineshige S., 1997, ApJ, 479, L97
Umemura M., Fukue J., Mineshige S., 1998, MNRAS, 299, 1123
Wada Y., Liou M. S., 1994, AIAA Paper, 94-0083
Wandel A., 1999, ApJ, 519, L39
Wandel A., 2002, ApJ, 565, 762

This paper has been typeset from a TEX/LATEX file prepared by the author.